

Changes in optical properties of YAG: Ce single crystals due to codoping and ionising radiation treatment

Sławomir M. Kaczmarek^a, Andrzej J. Wojtowicz^{b,c}, Winicjusz Drozdowski^b, Czesław Koepke^b, Krzysztof Wiśniewski^b, Jarosław Kisielewski^d, Ryszard Jabłoński^d, Marek Grinberg^e, Justyna Barzowska^e, B. Kukliński^e, Georg Zimmerer^f, Zbigniew Moroz^g, Henryk Rzewuski^h

^a Institute of Optoelectronics, Military University of Technology, 2 Kaliski Str., 00-908 Warsaw, Poland

^b Institute of Physics, N. Copernicus University, 5 Grudziądzka Str, 87-100 Toruń, Poland

^c Chemistry Department, Boston University, 590 Commonwealth Ave., Boston, MA 02215, USA

^d Institute of Electronic Materials Technology, 133 Wólczyńska Str., 01-919 Warsaw, Poland

^e Institute of Physics Research, University of Gdańsk, 57 Wita Stwosza Str., Gdańsk

^f Institut fuer Experimentalphysik der Universitat Hamburg, D 22761 Hamburg, Germany

^g Soltan Institute for Nuclear Studies, 05-400 Świerk

^h Institute of Nuclear Chemistry and Technology, 16 Dorodna Str., 03-195 Warsaw

ABSTRACT

Absorption, luminescence, ESR and ESA spectra and TL glow curves of YAG: Ce crystals codoped with Mg²⁺ ions and subjected to various treatments have been measured. The variations induced by irradiations in gamma and proton beams, and by thermal annealings under oxidation and reduction conditions point to large variations of the cerium ion valency.

The ESA spectra of Mg-free and Mg-codoped crystals are clearly different with the peak value in the YAG: Ce, Mg sample higher and shifted towards the shorter wavelengths. Although the TL glow curves reveal the existence of the same major traps in both materials, their role in the overall deexcitation process is strongly modified upon Mg-codoping.

Keywords: Absorption, luminescence, excited state absorption, thermoluminescence, glow curves, gamma irradiation, protons, additional absorption

SPIE, Vol. 3724, 339-345, 0277-786X/99/\$10.00

1. INTRODUCTION

Y₃Al₅O₁₂: Ce³⁺ (YAG: Ce³⁺) crystals have some characteristics highly desirable for an active material of the tuned solid state lasers¹. Among those are the 5d-4f transitions producing an emission of quantum efficiency close to unity in a broad band, extending from 500 to about 650 nm, the convenient broad pumping bands due to the allowed 4f-5d transitions in absorption and the properties of the YAG host matrix itself, such as excellent thermal and optical characteristics. However, the unacceptably high value of the excited state absorption (ESA) from the 5d₁ level, which overlaps the Ce³⁺ luminescence band, has prevented the lasing in YAG: Ce². Another application of YAG:Ce³⁺ crystal is in the area of medical imaging, tomography, gamma-cameras as scintillator material³.

The parameters of the YAG: Ce characterizing its performance as scintillator as well as a potential active laser medium depend, to a large extent, on its optical properties as well as on structural and radiation defects. These defects may be produced in the crystal during the growth or annealing procedures but they may also be created as a result of irradiation by ionising radiation^{4,9}.

The main goal of this work was to study structural and radiation defects in cerium doped YAG crystals influencing the crystal properties, important for scintillator and/or active laser medium applications.

*Further author information

S.M.K. (correspondence): Email: skaczmar@wat.waw.pl; Telephone: (022) 6859019

A.J.W. (correspondence): Email: andywojt@chem.bu.edu;

2. EXPERIMENTAL

YAG: Ce and YAG: Ce, Mg single crystals were grown by the Czochralski method at the Institute of Electronic Materials Technology¹⁰. The following samples were investigated: S1 - YAG: Ce (0.1 at. % Ce), S2 - YAG: Ce (0.2 at. %), S3 - YAG: Ce, Mg (0.2 at. %, 0.1 at. %) and S4 - YAG: Ce (0.05 at. %).

2.1 Irradiations

The samples were irradiated by gamma photons immediately after the crystal growth process at room temperature, and by protons after previous annealing at 1400° C in air. The gamma source of ⁶⁰Co with a strength of 1.5 Gy/s was used. The applied gamma doses were up to 10⁵ Gy.

For proton irradiation the beam from the C-30 cyclotron of SINS in Świerk was used. The proton energy was about 21 MeV, and the beam current at the sample was about 0.2 μA. The proton fluency was varied between 10¹³ to 10¹⁶ cm⁻².

2.2. Absorption, emission and excitation spectra measurements

1 mm thick samples were cut from the single crystals and subsequently polished on both sides. The optical transmission of those samples was measured before and after the thermal or radiation treatment, using LAMBDA-2 Perkin-Elmer spectrophotometer in the UV-VIS region and FTIR-1725 spectrophotometer in the IR region. After measuring the transmission, the absorption (K) and then, after the treatment, the additional absorption value ΔK were calculated according to the formula:

$$\Delta K(\lambda) = 1/d \ln (T_1(\lambda)/T_2(\lambda)), \quad (1)$$

where λ is the wavelength, d the sample thickness, T₁ and T₂ are the transmissions of the sample before and after an appropriate treatment procedure, respectively.

The room temperature fluorescence spectra were obtained under excitation of 275 nm wavelength by a Xenon lamp using LS-5B Perkin-Elmer spectrofluorimeter. The liquid helium spectra were measured in SUPERLUMI station at HASYLAB, Hamburg, Germany where the VUV range synchrotron radiation was used to excite the samples. Details of this setup can be found in Ref. [11].

2.3. ESA measurements

The ESA spectra were measured using an experimental setup described in Ref. [12].

2.4. Thermoluminescence measurements

The glow curves were recorded between 300 and 750 K using RISO TL/OSL system, model TL/OSL-DA-12¹³, at the heating rate of 1-5 K/s. Before the TL runs the samples were exposed to 196 keV β-rays from an Sr/Y-90 radioactive source for 2 s. The TL glow curves were taken in the Ar atmosphere.

2.5 ESR studies

The samples for ESR measurements had dimensions of 3.5x3.5x2 mm. The measurements were performed using BRUKER ESP-300 ESR (Band-X) spectrometer. The spectrometer was equipped with the helium flow cryostat type ESR900 Oxford Instruments. The ESR lines were observed before and after the UV illumination from the mercury lamp in the temperature range between 4 and 300 K. The microwave power was changed between 0.002 and 200 mW.

3. RESULTS

3.1 Basic spectroscopic measurements

Fig. 1 presents the absorption spectra of the samples S1...S4 in the range between 150 and 650 nm. The spectra show Ce transitions with maxima at the wavelengths of 224 nm, 266 nm, 340 nm and 458 nm. The fifth transition, at 211 nm, was already described in Ref. [1]. The Mg-codoped sample (S3) shows a shift of the short wavelength absorption edge toward the longer wavelengths by about 100 nm in comparison to other samples. The samples for which Ce concentration exceeds 0.1 at. %: (S2 and S3) show a distorted absorption spectrum which, upon subtraction of the spectrum measured for the lightly doped sample, reveals two additional peaks at 448 and 473 nm (see ΔS₂₁≡K_{S2}-K_{S1} and ΔS₂₃≡K_{S2}-K_{S3} curves) of no direct physical significance.

In Fig. 2 we present the luminescence spectrum of the sample S1 in the UV-VIS range, which is typical for S2 and S3 samples also. In addition to the well-known broad luminescence band due to transitions from the lowest 5d state (5d₁) to the 4f ground state of the Ce³⁺ ions, there are also sharp lines between 350 nm and 500 nm most likely due to the f-f transitions

of Tb^{3+} ions (unintentional impurity). The luminescence spectrum of the S4 sample that was grown independently of others, does not show any presence of those unexpected emissions.

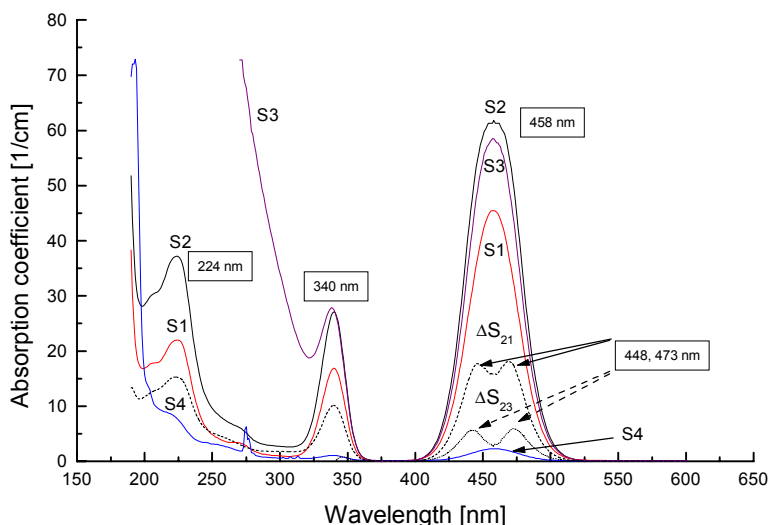


Fig. 1. Absorption and differences in the absorption of the four investigated crystals.

The low temperature (liquid helium) luminescence spectra of the S3 sample, measured for three values of the excitation light wavelength λ_{ex} of 170 nm, 270 nm and 325 nm, and shown in Fig. 3, contain the same lines as those observed earlier for the sample S1 (Fig. 2), at 386, 417 and 440 nm. Moreover, for the $\lambda_{ex}=325$ nm there is one additional sharp emission line at 360 nm. This confirms Fig. 4, where the excitation spectrum measured at liquid helium temperature for the S3 sample is presented, showing maximum at 325 nm. The origin of the emission at 360 nm remains unclear. Note that the difference between the excitation spectra of 360 nm and 520 nm emissions clearly indicates that the origin of the 360 nm is not due to Ce^{3+} ions. The peak at 175 nm, seen in the excitation spectra, is probably of the excitonic origin and, as such, must be close to the forbidden energy gap of the material. The excitation spectra for 265 nm emission of the Fig. 4 suggests the excitonic origin of that emission (exciton trapped at the defect site in the YAG host material).

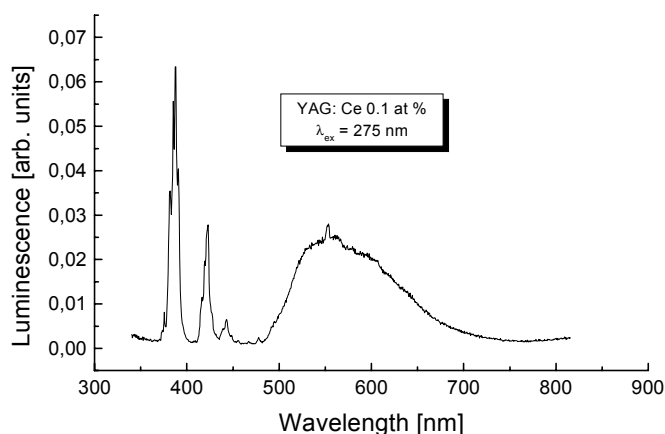


Fig. 2. Luminescence spectrum of YAG: Ce (0.1 at %) - S1 sample. $\lambda_{ex}=275$ nm.

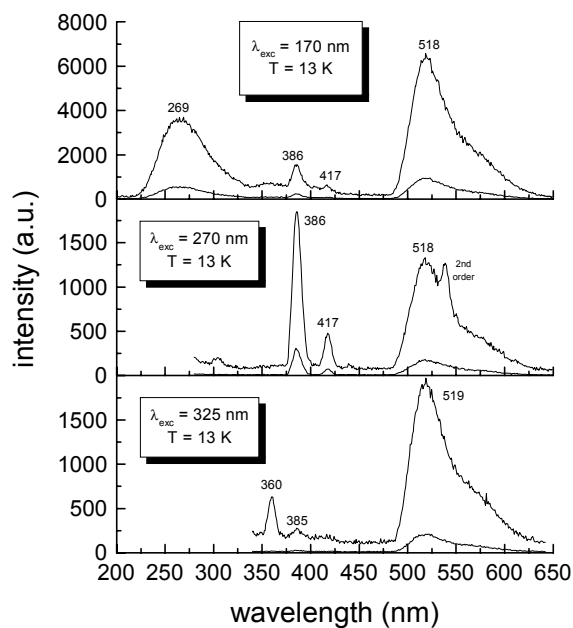


Fig. 3. Liquid helium emission spectra of YAG: Ce, Mg for $\lambda_{ex}=170$, 270 and 325 nm. Resolution 6.4 nm.

In Fig. 5 we show the results of the additional absorption measurements, obtained with use of the equation (1) for the S3 sample after different treatments. These spectra correspond, for instance, to the increase of Ce^{3+} absorption ($Ce^{4+}+e^{-}\rightarrow Ce^{3+}$) after γ -irradiation (curves 1, 3, 5), or the decrease of the Ce^{3+} absorption after annealing in the reducing atmosphere (N_2+H_2 mixture) at 1200°C for 3h (may be due to $Ce^{3+}\rightarrow Ce^{1+}$ transition) - curve 4 (or curve 2 after annealing at 400°C in the air).

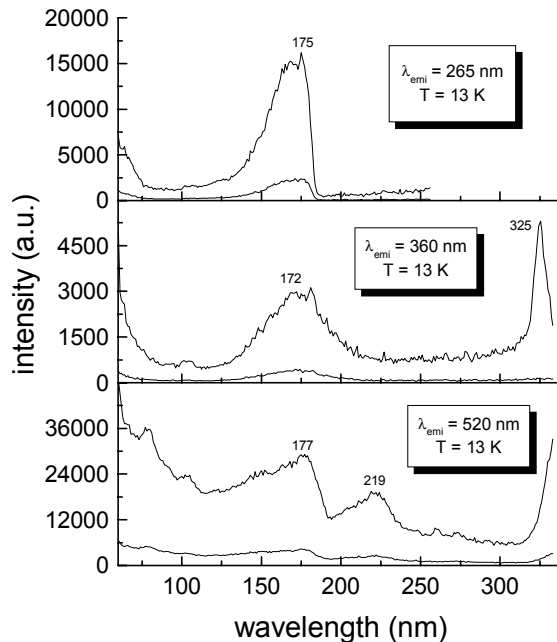


Fig. 4. Liquid helium excitation spectra of YAG: Ce (0.2 at. % Ce, 0.1 at. % Mg) for $\lambda_{emi}=265$, 360 and 520 nm, corrected for the setup characteristics. Resolution 0.3 nm.

In the absorption difference spectrum, ΔS_{23} (curve 7), we see two peaks described previously. Interestingly, no such effects are observed in the Ce^{3+} absorption band after gamma irradiation in YAG: Ce (0.05 at. %) - sample S4. This effect is due to the shifting of the absorption band caused by higher concentration of Ce^{3+} ions. The results of proton irradiation are very similar to γ -irradiation results (curve 6).

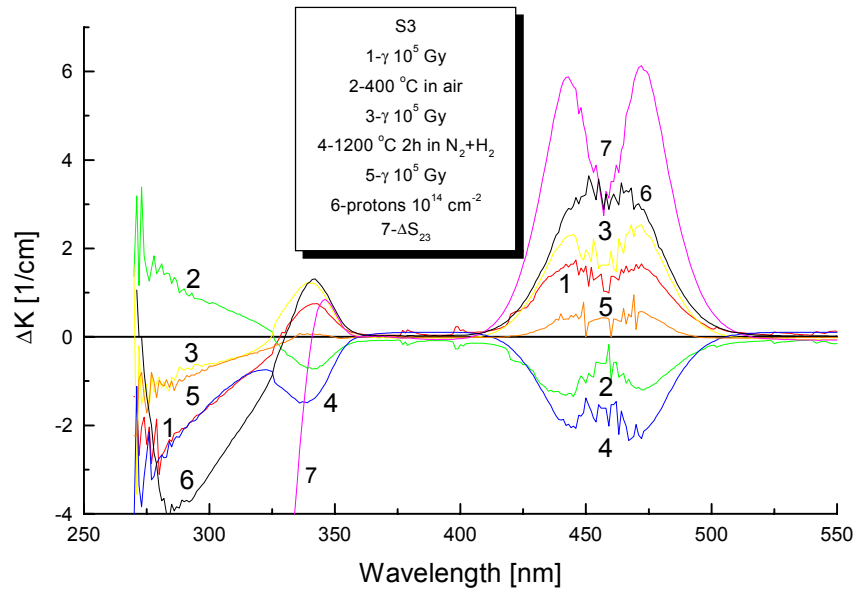


Fig. 5. Additional absorption of YAG: Ce, Mg crystal - sample S3 subsequently: (1) - after γ - irradiation with a dose of 10^5 Gy, (2) - after annealing at $400^\circ C$ for 3h in the air, (3) - after γ - irradiation with a dose of 10^5 Gy, (4) - after annealing of the crystal in reducing atmosphere at $1200^\circ C$ for 2h, (5) - after γ - irradiation with a dose of 10^5 Gy, (6) - after proton irradiation with a fluency of $10^{14} cm^{-2}$ and, (7) - difference between absorption of S2 and S3 samples.

3.2 ESA measurements

The YAG: Ce spectrum closely resembles the literature curve, with the characteristic tail on the high energy side assigned to the transient color centers^{17, 18}. On the other hand the YAG: Ce, Mg spectrum, is very different, with a much higher intensity, a shifted maximum and a different shape. It goes without saying that this spectrum *is not* due to Ce ions. It rather must reflect the difference between two samples created by the Mg-codoping and, possibly, to the increased population of some traps.

3.3 Thermoluminescence measurements

In the experimental glow curves of YAG: Ce and YAG: Ce, Mg one can distinguish four glow peaks at about 330, 410, 460, and 550, which correspond to four electron traps. The results of the fitting procedure (described in detail in Ref. [19]) give the calculated depths of the above traps equal to about 1.2 eV. The Mg-codoping does not influence the trap distribution at all. However, contrary to expectations, the TL signal is much lower (100 times) suggesting that traps, particularly the one glowing at about 410 K, are suppressed. Since the relative concentrations of various traps are also changed, the effect can not be exclusively due to the thinkable competition for holes between the Ce ions and the Mg-related defect responsible for the electron-filled level 3.5 eV below the conduction band, identified previously¹⁷.

3.4. ESR studies

ESR spectrum for Ce: YAG or Ce, Mg: YAG shows typical orthorhombic symmetry of the rare-earth ion substituted in the position of yttrium. The interaction of the electrons with the magnetic field H is given by the following Hamiltonian :

$$H = \beta(L + 2S)H, \quad (2)$$

$$\text{or } H = \beta H g S,$$

where: β - Bohr magneton, h - Planck constant, L - orbital quantum number, $S=1/2$. The Lande factor, g , is given by:

$$g^2 = g_x^2 l^2 + g_y^2 m^2 + g_z^2 n^2, \quad (3)$$

where: l , m , n are directional cosines. The components of g -factor are presented in Table 1, where literature values are also given.

Table 1. Experimental values of the g -factors.

g_x	g_y	g_z	Literature
1.872	0.9098	2.738	[21]
1.8729	0.91039(2)	2.73814(3)	this paper

Pure YAG does not show any ESR signal. The ratio of ESR intensities for S1 and S2 crystals was about 1.8 ± 0.3 . ESR intensity for S2 crystal was comparable with this for S3.

Irradiation of all investigated samples by UV light from mercury lamp at 14 K causes about twice increase in the intensity of the ESR lines. Annealing of the crystal at 200 K leads to the decrease in ESR intensity by 15%, annealing at 240 K leads to the next decrease by about 20% and annealing of the crystal at 270 K causes the return to the situation before the irradiation. The above process is almost totally reversible.

4. CONCLUSIONS

For all cerium concentrations one can see characteristic Ce^{3+} absorption bands peaked at 211, 224, 266, 340 and 458 nm, and the absorption edge starting at 190 nm related to the band to band transition in YAG crystal. The band gap of the material, however, as evident from the excitation spectrum of the Ce^{3+} emission which shows the excitonic peak at 175 nm, must be at least 7.1 eV. For the sample codoped with Mg there is an additional absorption, which effectively shifts the absorption edge to about 300 nm.

This absorption must be due to the transition between the Mg-related defect state and the conduction band of the YAG host material and, therefore, its position allows to roughly estimate the energy of the Mg induced defect level to be about 3 eV above the valence band. The position of the Ce^{3+} ground state level calculated from the band gap and the photoconductivity measurements of Pedrini *et al*¹⁵ appears to be about 3.3 eV above the valence band, slightly higher than the Mg defect level. The presence of the acceptor like, therefore partially empty level below the Ce^{3+} level explains the observed decrease of the Ce^{3+} concentration in YAG: Ce, Mg, as evidenced by the absorption spectra shown in Fig. 1.

The excitation and emission spectra of the YAG: Ce and YAG: Ce, Mg crystals measured at liquid helium temperature reveal the presence of the inadvertent impurity, most likely Tb, in S1...S3 samples. In addition there is an emission band centered at 360 nm which also, most likely, is due to some other uncontrolled impurity.

The increase of the Ce^{3+} concentration after irradiation of all the studied samples with gamma, electron and proton beams (Fig. 5), as well as the increase of the ESR signal due to the Ce^{3+} upon irradiation with the UV light from the mercury lamp, consistently suggest the presence of the Ce^{4+} ions in all of our samples.

There are, nevertheless, two contradictory effects associated with the codoping of YAG: Ce crystals with Mg^{2+} ions. They are: the increased ESA (suggesting a higher concentration of some kind of color centers and/or substantial populations of some traps) and the reduced TL intensity (suggesting a lower concentration of traps). To resolve this apparent contradiction we note that the excimer laser pump at the wavelength of 308 nm is absorbed mostly by the Mg-related defects identified previously. Only a relatively small fraction of the pump beam intensity is used to excite the Ce-ions.

The large changes in the ESR signal observed upon UV irradiation from the mercury lamp have been already discussed. Although no enhancement has been observed for the Mg-codoped sample, the ESR effect appears otherwise similar to the ESA increase under the excimer laser irradiation and has, most likely, the same underlying mechanism; namely, the transfer of electrons from the low lying defect levels to the conduction band and then to Ce^{4+} ions.

5. ACKNOWLEDGMENTS

This work was sponsored by the Polish Committee for Scientific Research (projects no 2 P03B 003 13 and 2 P03B 049 14). The authors would like to thank Dr. M. Kirm from HASYLAB, Hamburg, Germany for assistance at LHeT and VUV experiments, and Prof. H.L. Oczkowski and K.R. Przegiętka from Nicholas Copernicus University for their help in thermoluminescence measurements. Thanks are also due to Dr T.M. Piters from Universidad de Sonora, Mexico for the fitting procedure we used for TL analysis.

6. REFERENCES

1. T. Tomiki, H. Akamine, M. Gushiken, Y. Kinjoh, M. Miyazato, T. Miyazato, N. Toyokawa, M. Hiraoka, N. Hirata, Y. Ganaha and T. Fudemma, „Ce³⁺ centers in Y₃Al₅O₁₂ (YAG) single crystals”, *J. Phys. Soc. Japan* **60**, p. 2437, 1991.
2. D.S. Hamilton, S.K. Gayen, G.J. Pogatshnik, and R.D. Ghen, *Phys. Rev.* **B 39**, p. 8807, 1989.
3. A. A. Kaminskii, „Laser crystals”, p. 215, Moskwa, *Nauka*, 1975.
4. G. A. Slack, S. L. Dole, V. Tsoukala and G. S. Nolas, „Optical absorption spectrum of trivalent cerium in Y₂O₃, Ba₂GdTaO₆, ThO₂ and related compounds”, *J. Opt. Soc. Am.* **B11**, p. 961, 1994.
5. W. M. Yen, S. Basun, U. Happek and M. Raukas, „Luminescence and photoconductivity of cerium compounds”, *Acta Physica Polonica* **A90**, p. 257, 1996.
6. S.M. Kaczmarek, D.J. Sugak, A.O. Matkovskii, Z. Moroz, M. Kwaśny, A.N. Durygin, „Radiation induced recharging of cerium ions in Nd, Ce:Y₃Al₅O₁₂ single crystals”, *Nucl. Instr. Meth.* **B 132**, p. 647, 1997.
7. S. M. Kaczmarek, M. Kwaśny, M. Malinowski, Z. Moroz, "Excitation-emission spectra of laser materials for UV-VIS range", *Proc. SPIE* **3186**, p. 51, 1997.
8. S. M. Kaczmarek, M. Kwaśny, A. O. Matkovskii, D.J. Sugak, Z. Mierczyk, Z. Frukacz, J. Kisielewski, "Effect of the increase of Ce³⁺ ions content after gamma irradiation of Ce and Ce, Nd doped YAG single crystals", *Biuletyn WAT* **8**, p. 93, 1996.
9. S. M. Kaczmarek, M. Kwaśny, J. Kisielewski, Z. Moroz, A.O. Matkovskii, D.J. Sugak, „Gamma-induced effect of recharging: Ce⁴⁺→Ce³⁺ in Ce and Nd doped YAG crystals”, *Proc. SPIE* **3178**, p. 279, 1997.
10. S.M. Kaczmarek, J. Kisielewski, R. Jabłoński, Z. Moroz, M. Kwaśny, T. Łukasiewicz, S. Warchoń, J. Wojtkowska, „Crystal growth and optical properties of Ce and Mg doped YAG crystals”, *Biuletyn WAT* (in Polish) **7/8**, p. 113, 1998.
11. G. Zimmerer, „Status Report on Luminescence Investigations with Synchrotron Radiation at HASYLAB”, *Nucl. Instr. Meth.* **A308**, p. 178, 1991.
12. Cz. Koepke, K. Wiśniewski, M. Grinberg, D.L. Russell, K. Holliday, and G.H. Beall, *J. Lumin.* **78**, p. 135, 1998.
13. L. Botter-Jensen, *Nucl. Tracks Rad. Meas.* **14**, p. 177, 1988.
14. W.J. Miniscalco, J.M. Pellegrino, and W.M. Yen, *J. Appl. Phys.* **49**, p. 6109, 1978.
15. C. Pedrini, F. Rogemond, D.S. McClure, *J. Appl. Phys.* **59**, p. 1196, 1986.
16. B.Di Bartolo, „Optical Interaction in Solids”, p. 112, Wiley, New York, 1968
17. K. Wiśniewski, Cz. Koepke, A.J. Wojtowicz, W. Drozdowski, M. Grinberg, S.M. Kaczmarek, J. Kisielewski, “Excited state absorption in Ce and Mg doped Yttrium Aluminum Garnet”, *Acta Physica Polonica*, in print.
18. K.S. Bagdasarov, L.B. Pasternak, and B.K. Sevastyanov, *Sov. J. Quantum Electron.* **7**, p. 965, 1977.
19. W. Drozdowski, K.R. Przegiętka, A.J. Wojtowicz, H.L. Oczkowski, „Charge traps in Ce-doped CaF₂ and BaF₂”, *Acta Physica Polonica A*, in print.
20. A. Abragam, B. Bleaney, „Electron Paramagnetic Resonance of transition Ions”, pp. 60-66, Clarendon Press, Oxford, 1970.
21. H.R. Lewis, „Paramagnetic Resonance of Ce³⁺ in Yttrium Aluminum Garnet”, *J. Appl. Phys.* **37**, p. 739, 1966.
22. Y. Suzuki, T. Sakuma, M. Hirai, „UV emission from the second lowest 5d state in Ce³⁺: YAG”, *Materials Science Forum* **239-241**, p. 219, 1997.